

# A microfluidic device for continuous cancer cell culture and passage with hydrodynamic forces

Liyu Liu,<sup>ac</sup> Kevin Louterback,<sup>bc</sup> David Liao,<sup>ac</sup> David Yeater,<sup>d</sup> Guillaume Lambert,<sup>ac</sup> André Estévez-Torres,<sup>ac</sup> James C. Sturm,<sup>bc</sup> Robert H. Getzenberg<sup>d</sup> and Robert H. Austin<sup>\*ac</sup>

Received 23rd February 2010, Accepted 8th April 2010

First published as an Advance Article on the web 27th April 2010

DOI: 10.1039/c003509b

We demonstrate a novel and robust microfluidic chip with combined functions of continuous culture and output of PC-3 prostate cancer cells. With digital controls, polydimethylsiloxane (PDMS) flexible diaphragms are able to apply hydrodynamic shear forces on cultures, detaching a fraction of attached cancer cells from the surface for output while leaving others for reuse in subsequent cultures. The fractions of detached cells and remaining cells can be precisely controlled. The system has not only the advantages of small size, high cell culture efficiency, and digital control, but also of simple fabrication at low cost, easy operation and robust performance. The chip performs 9 passages during 30 days of continuous culture and shows promise as a durable design suitable for long-term cell output.

## Introduction

Cancer is a common cause of chronic and terminal human disease.<sup>1</sup> Cancer progression consists of cells invading local tissues and metastasizing to other parts of the body *via* the blood stream or the lymphatic system.<sup>2</sup> Prostate cancer is a typical cancer in men. Due to the nature of the disease, prostate cancer has become known as the inevitable cancer; most men will contract this disease if they live long enough. Currently, there are numerous *in vitro* models that can be used for the study of prostate cancer, one of which is the cell line PC-3. PC-3 cells are a prostate epithelial cancer cell line derived from a human prostatic adenocarcinoma bone metastasis.<sup>3</sup> This aggressive, poorly differentiated adenocarcinoma cell line is an ideal model for investigating the changes in advanced prostatic disease and its reaction to various therapies.

Because of the devastating cost of current cancer therapies, the need to study and hopefully cure cancer is a driving force in today's biomedical research. Unlike traditional macro-research methods relying upon homogenous environments for tumors and cancer cells, microfluidic technologies have shown incomparable advantages in cancer studies in micro- and nano-scales in recent years. Compared to traditional methods, microfluidic chips provide more accurate manipulation of individual cancer cells. They also provide dynamic control of micro-environmental parameters, such as pH, CO<sub>2</sub>/O<sub>2</sub> concentrations, *etc.* Furthermore, a single cell can be easily tracked, captured and directed for specific biological studies. A microfluidic platform for circulating tumor cells and identifying related viable tumor-derived epithelial cells has been reported previously.<sup>4</sup> To study

metastasis, a multi-step microfluidic device is used for generating deformation and extravasation of primary tumor cells.<sup>5</sup> Additional research has approached targeted cancer therapeutics by imitating gradients in micro-environments.<sup>6</sup> One can anticipate that microfluidic technology will have broad implications in research in cancer biology, as well as in clinical management, including in the detection, diagnosis and monitoring of cancer cells at micro-scales.

*In vitro* growth of a cell culture is the first step for most research laboratory studies of cancer. Microfluidic chips have mimicked *in vivo* environments controllably.<sup>7,8</sup> In some microfluidic systems developed for repeated cell culture, trypsin is used for the periodic passage of cells.<sup>9</sup> However, the trypsin used to detach fixed cells digests coatings on bio-functionalized surfaces, which in turn reduces chip performance during continued use and therefore, potentially limits the number of repeated cell culture passages.<sup>10</sup> Another study showed how cancer cells can be deformed and detached using hydrodynamic forces created in micro-channels at varying flow rates and acceleration.<sup>11</sup> Micro-channel geometry has also been shown to control cell adhesion.<sup>12</sup>

In this paper, we present a microfluidic chip for PC-3 prostate cancer cell continuous culture and passage on polydimethylsiloxane (PDMS) and bio-functionalized glass coatings. The chip's inner integrated PDMS diaphragms detach adherent cells purely through hydrodynamic shearing forces. With this method, cell passage ratios can be precisely chosen allowing a specific number of cells to be preserved for subsequent culture. The ability to passage cells without chemical reagents not only simplifies the chip's operation, but also makes it suitable for multi-passage experiments when combined with durable bio-coatings. This system creates a simple and robust cancer cell culture and output technology requiring less human intervention and reducing opportunities for contamination.

PDMS is now a staple of the microfluidics community, thanks to its simple fabrication process and material attributes, such as gas permeability, optical transparency, biocompatibility and flexibility. It is widely used for biological studies, for instance, as

<sup>a</sup>Dept. of Physics, Princeton University, NJ, USA. E-mail: austin@princeton.edu

<sup>b</sup>Dept. of Electrical Engineering, Princeton University, NJ, USA

<sup>c</sup>Princeton Institute for the Science and Technology of Materials, Princeton University, NJ, USA

<sup>d</sup>Dept. of Urology, Oncology, Pharmacology and Molecular Sciences, Johns Hopkins University School of Medicine, MD, USA

a platform for DNA amplification<sup>13</sup> and cell culture.<sup>14</sup> Because of its flexibility, transformations with movements of PDMS diaphragms can be accurately controlled with digital signals, providing corresponding mechanical forces for cell passage.<sup>15</sup>

## Materials and methods

### Device design and fabrication

The chip is constructed of PDMS and glass. Fig. 1(A) shows a schematic diagram of the microchip's multi-layered structure. Cancer cells are cultured in the lower layer and cell passage is controlled by gas channels in the upper layer. The lower layer is a combination of a thin film of PDMS with micro-channels on a glass substrate. A 10 mm × 9 mm square chamber is located in the middle. The chamber has 500 micron high PDMS walls and a glass bottom in which cells can be cultured and passaged. Cells and culture media are introduced into the chamber from the upper layers *via* metallic tubes. The middle layer, a 32 micron thick elastic PDMS diaphragm inserted between the lower and upper layers, serves to separate the fluids in the two layers, as well as to transmit forces from the upper layer to the lower layer *via* its vertical elastic deformations. The upper PDMS layer possesses four identical rectangular chambers (displayed in green) in the middle, which are 10 mm long and 2 mm wide. The chambers are separated by 500 micron gaps. The first and third chambers, as seen going from left to right, are attached to one external gas source. The remaining second and fourth chambers are attached to a second external gas source. Combined with the thin diaphragm underneath, the chambers are capable of generating dynamic shearing forces in the lower chamber in response to adjustments to the gas sources. On both sides, there are two L-shaped channels deployed for independent valve control (displayed in yellow), which seal the lower cell culture chamber during the cell passing process. Metallic tubes are

installed to conduct cells, culture media and control gas inside the chip, as indicated in the figure. The lower left inset of Fig. 1(A) is an image of the microfluidic chip placed in an acrylic operation platform.

Fig. 1(B) shows our fabrication procedure. PDMS is first poured onto a glass substrate and spun at 100 rpm for 60 seconds, creating a 500 micron thick PDMS film.<sup>16</sup> After PDMS is fully cured, micro-channels for cells are cut through the PDMS layer (step 2). Simultaneously, a 32 micron PDMS diaphragm is spun onto a glass substrate and cured. Then the diaphragm, together with the substrate, is flipped over, as shown in the blue dashed line box on the right. In step 3, the diaphragm layer is aligned and bonded with the cell channel layer from step 2. The diaphragm is then lifted off from the upper glass substrate (step 4). At the same time, a 500 micron thick acrylic pattern cut by a laser is stuck to an acrylic board as a mold (shown in the red dashed line box). PDMS is then poured onto the mold, fully covering this pattern. After curing, the PDMS layer is lifted off. In the last step, this PDMS layer containing gas channels is combined with the multi-layer assembly obtained from step 4, finishing the chip assembly.

### Culture surface coating with gelatin

Components of the extracellular matrix (ECM) are often used to coat glass or plastic surfaces to enhance cell attachment, growth and development. Here, we use gelatin (Stemcell Tech, Vancouver, Canada) to coat the glass bottom of the culture chamber for the culturing of PC-3 cells. The gelatin coating, a process requiring three steps, is performed before the layers of the chip are assembled. First, 500  $\mu$ L of gelatin buffer is pipetted into the culture chamber. Subsequently, the culture chamber layer is placed in an air hood at room temperature for one hour. Finally, the remaining gelatin is aspirated thoroughly by pipette and the

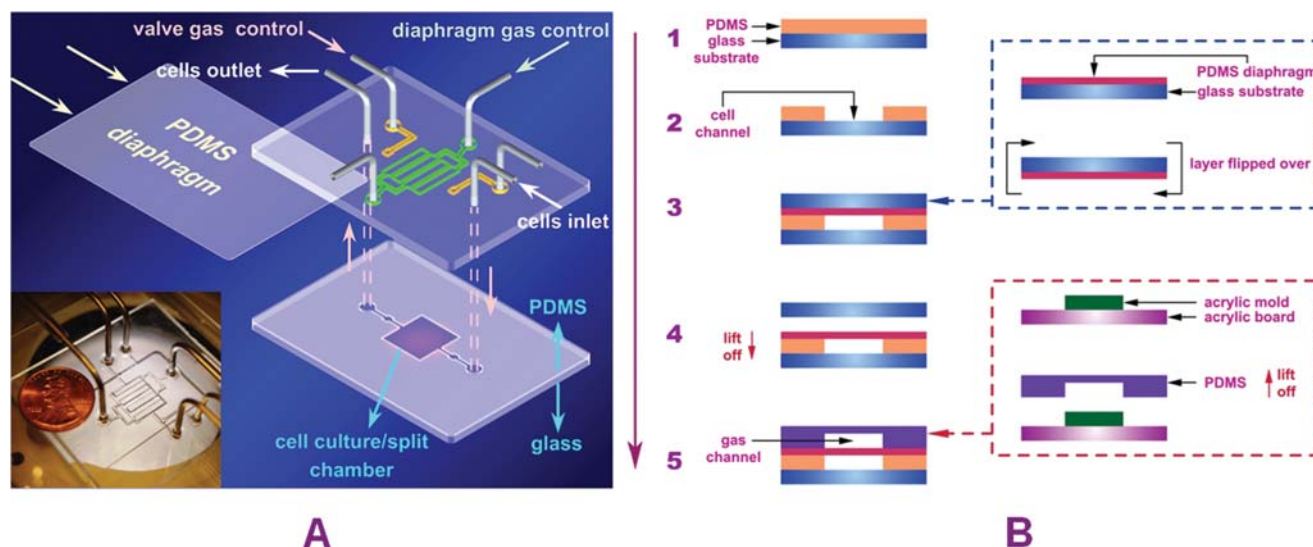


**Fig. 1** (A) Schematic illustrations of the 3D layered structure of the PDMS-based microfluidic chip for the continuous culture and passage of PC-3 cancer cells. The cell culture chamber with microfluidic channels in PDMS layer combined with glass substrate is located on the lower layer, while the air channels for cell passage controls are on the upper layer. A thin diaphragm is sandwiched between the upper and lower layers, by which air forces are transmitted to manipulate the passing process. The left lower inset shows the chip with media and gas supply tubes linked, placed beside a one-cent coin. (B) A process-flow diagram illustrates the fabrication procedure of the micro-device with multiple layers. Description of the steps is in the text.

layer is left in the hood for an additional hour to allow the chamber surface to dry completely before chip assembly resumes.

### PC-3 cell preparation

The PC-3 cells were obtained from the American Type Culture Collection (ATCC-CRL 1435, Manassas, VA). The cells were cultured in Dulbecco's Modified Eagle Medium (DMEM) (Fisher #MT10017CV) supplemented with 10% Fetal Bovine Serum (Gemini #900108) and 1% penicillin/streptomycin (Sigma #P4333). Cells were cultured in a humidified atmosphere at 37 °C with 5% CO<sub>2</sub>. A monolayer grew to approximately 80% confluency before being passaged. In cancer cell growth, it is not optimal to allow cells to grow to complete confluence. Cells grown to confluence tend to form cell aggregates as well as move out of the exponential growth phase.

### On-chip cell culture and passage process

The process of on-chip PC-3 continuous culture, passage and output is demonstrated by a flow chart in Fig. 2. Before loading into the microfluidic chip, cells were grown to approximately 80% confluency and collected for experiments by trypsinization using a 0.25% Trypsin–EDTA (Mediatech Inc., Manassas, VA) solution. Cell suspensions were then centrifuged at 1500 rpm for 5 minutes. Pelleted cells were resuspended in DMEM.

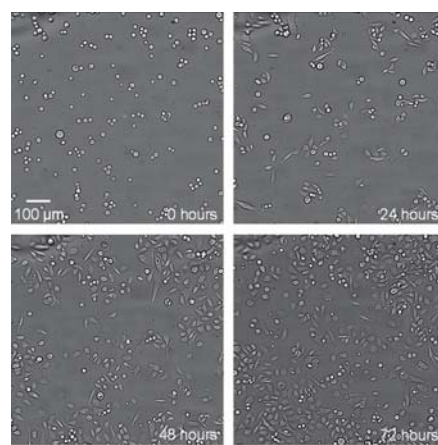
We steadily seeded cells into a chip at 50  $\mu\text{L min}^{-1}$  through a syringe pump (Chemyx Inc., Stafford, TX). Approximately 10<sup>4</sup> cells were plated in each device. In previous experiments, we found that cells appeared unhealthy when we kept chips at 37 °C with 5.0% CO<sub>2</sub>. The chip design, which includes multiple structures with thick PDMS as well as the glass substrate, does not allow DMEM media sealed within the chamber to receive ample CO<sub>2</sub> for the optimized culture of cells, despite the gas permeability of PDMS. To counter this, we kept the chip in an incubator at 37 °C with 7.5% CO<sub>2</sub> concentration.

After 72 hours in culture, when cells reached approximately 80% confluency, we passaged cells using the built-in features of the chip. We supplied fresh media to the culture chamber to flush out unhealthy and dead cells at a rate of 100  $\mu\text{L min}^{-1}$ . We then stopped flow of media and activated the two valves in the upper

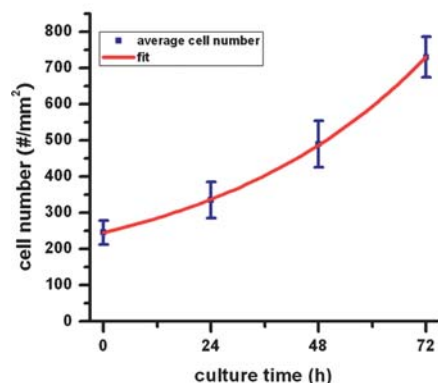
PDMS layer to completely seal the middle culture chamber. The passing diaphragms applied alternating forces, detaching a selectable number of the cells from the surface. After completing the passing process, we reopened the valves, allowing the flow of DMEM media to flush detached and floating cells out of the culture chamber. The remaining cells were allowed to incubate in fresh media until confluency of approximately 80% was reached. The process could then be repeated.

### Results and discussion

Fig. 3 illustrates PC-3 cell culture proliferation during the first 72 hours after loading. We took bright-field images of cells cultured inside microfluidic chips using a Nikon TE-2000 inverted microscope. We took pictures every 24 hours in separate chips; Fig. 3(A) shows a representative sequence of pictures from one chip. Each picture covers a 900 micron  $\times$  900 micron region. At 0 hours, just after loading, cells floated inside the chamber in round shapes. After incubation for 24 hours, most of the cells had settled and attached to the bottom surface; some of these had begun to spread out. We noticed a small increase in the number



A



B

### PC-3 cell preparation

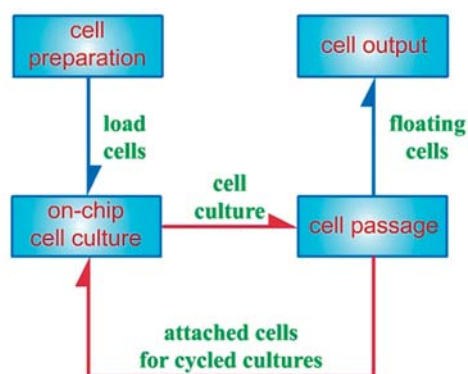


**Fig. 2** Diagram of the cancer cell culture and passage process. The chip is able to perform repeated cell cultures and simultaneously output cells as shown.

**Fig. 3** (A) Pictures of cell growth inside the culture chamber, where number increases gradually with time (0, 24, 48 and 72 hours). (B) Cell number plotted as a function of time. Blue dots are average cell numbers collected from culture chambers in three different chips and fit to an exponential growth model (red line).

of cells. After 48 hours, most cells spread out and attained long spindle shapes. At this point, the number of cells increased significantly. At 72 hours, the cells had grown significantly to near confluence. We counted cells in three different chips to derive cell numbers as a function of time. In Fig. 3(B), the average number of cells is plotted in blue as a function of culture time. The blue points are the average numbers of cells with error bars representing the corresponding standard errors of means. The increase in cell number fits an exponential growth model (red line), and the total number of cells nearly triples during the 72 hour incubation period. At this time, the chips contained a number of cultured cells adequate for a subsequent passage process.

Cancer cell passage is a core function of our chip design. The advantage of our approach is that the chip uses micro-scale shearing forces for detaching adherent cells without the use of chemical reagents, such as trypsin. Hence, this trypsin-free passage no longer consumes the gelatin coating, which enables multiple uses of the growth surface. DMEM supplemented with Fetal Bovine Serum and antibiotics is the only reagent needed, which allows for a simple, robust system. Fig. 4(A) reveals the working mechanism of the diaphragms used for cell passage inside the chip. The left picture is a cross-section view of two adjacent diaphragms in the layered chip structure. There are four electromagnetic (EM) valves, which are divided into two groups

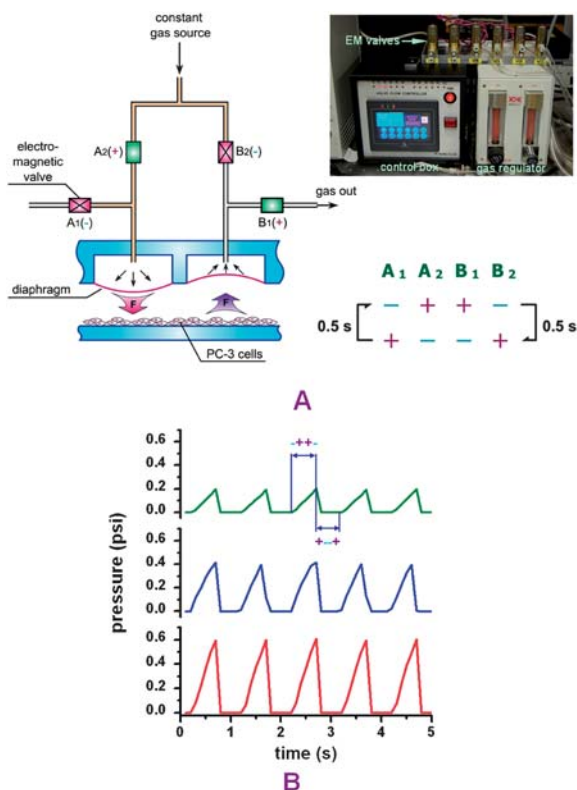


**Fig. 4** (A) Structures and mechanisms of PDMS diaphragms in passing cancer cells with electromagnetic valves. The photograph shows the control box as well as the gas regulator, which controls the EM valves. (B) Different variations of gas pressures for left diaphragm (in (A)) actuations during cell passing progress. The maximum pressure ranges from 0.2 to 0.6 psi.

controlling the diaphragms individually. The left diaphragm is controlled by the  $A_1$  and  $A_2$  valves, while the right is controlled by the  $B_1$  and  $B_2$  valves, both of which share the same gas source. PC-3 cells are cultured on the gelatin-coated glass surface beneath the diaphragms. When  $A_1$  is closed and  $A_2$  is open, compressed gas will be forced into the left diaphragm chamber causing the pressure to accumulate above the diaphragm, pushing it downward. The volume of the medium decreases as the diaphragm is compressed, creating a hydrodynamic shearing force capable of detaching the cells from the gelatin coated growth surface. Simultaneously in the right diaphragm, the reverse process occurs;  $B_2$  is closed and  $B_1$  is open. In this case, the compressed air is blocked by  $B_2$  and the gas flows externally through  $B_1$ , decreasing the pressure within the channel, thereby pulling the diaphragm upwards. These diaphragm repelling and imbibing actions are produced continuously *via* synchronized electrical signals, allowing the volume of the medium inside the chamber to remain constant, as shown in Fig. 4(A). As the figure shows, we switch every 0.5 seconds between two groups of digital signals operating the four valves, *e.g.*, the direction of forces under each diaphragm changes at a fixed 2 Hz frequency. The upper right inset is the complete setup for the above diaphragm operations. There are six EM valves, four of which are used in this experiment and operated by signals from the lower control box. The gas regulator (Okolab Inc, Ottaviano, Italy) linked to the valves at the side provides constant compressed air with pressure controls.

A computer recorded diaphragm pressure measured using a manometer (Sper Scientific, Scottsdale, AZ). The manometer connected to the left chamber in Fig. 4(A). When we applied the first signal ( $- + + -$ ) to the valves, the pressure inside the chamber rose. When we applied the second signal ( $+ - - +$ ), pressure decreased to zero. Fig. 4(B) shows the triangle waves of pressure for maximum pressures of 0.2, 0.4 and 0.6 psi, in green, blue, and red, respectively. The maximum pressure is determined by the gas source. Higher input gas pressure results in higher maximum pressure inside the diaphragm. The triangle waves in Fig. 4(B) remain stable in amplitude and shape during the hundreds of cycles necessary for cell passage. In this way, the diaphragms generate reliable actuated forces for controlled rates of cell detachment during cell passage.

Hydrodynamic forces are the key for detachment of cells during the passage process. Fig. 5 shows a numerical simulation that is representative of the fluid motion in the device during passage. Flow was simulated in a numerical solver (COMSOL) with boundary conditions as shown in the central figure. Fig. 5(B) shows the magnitude of the velocity field, where the depressed diaphragm moves downward at 500 microns  $s^{-1}$  while the raised membrane moves upward at the same rate. Fig. 5(A) is a vector-field plot of the 1000 micron region surrounding the lowest point of the diaphragm. The simulation indicates that the fluid moves at greatest speed under the diaphragm and that fluid moves primarily in the horizontal direction, transverse to the diaphragm surface.

We model cells as 15 micron spheres and estimate hydrodynamic forces 10 microns above the surface of the substrate (white dashed line in the central figure). We compare the relative strengths of two forces: shear force from gradients in the lateral velocity and drag force from the vertical velocity. We neglect

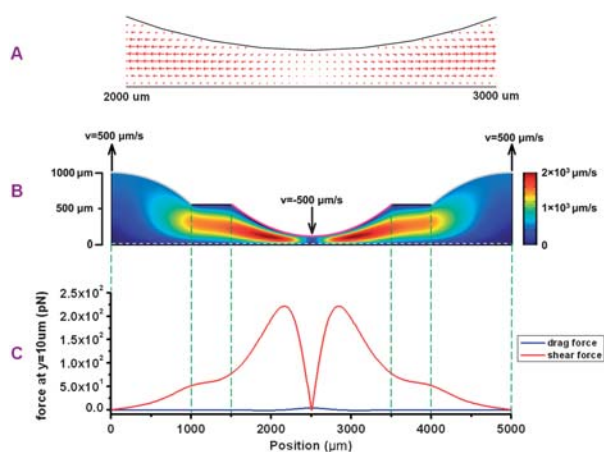


**Fig. 5** Numerical simulation using COMSOL of fluid motion inside the device during passage. The depressed membrane moves downward at 500 microns  $s^{-1}$  while the raised membrane moves upward at the same rate. (A) Vector-field plot of the 1000 micron region surrounding the lowest point of the diaphragm. (B) Magnitude of the velocity field. (C) Estimates of shear and drag forces experienced by cells 10 microns above the culture surface.

drag force from the lateral velocity assuming that confluent cells shield each other from lateral flow. The shear force is estimated by multiplying the shear stress at 10 microns above the surface with the surface area of a cell. The drag force in the vertical direction is similarly estimated with the Stokes' drag relation using the vertical velocity field. Fig. 5(C) shows a plot of the magnitude of these forces as a function of position in the device. Drag forces are more than an order of magnitude weaker than shear forces. The shear force is greatest under the membrane, dropping from a peak value of 221 pN to a level value of about

50 pN in the open area between diaphragms. This results in relatively fewer cells detached in these open areas. As the diaphragms switch back and forth, cells underneath the diaphragms experience stronger shear forces and are more prone to detachment from the surface.

Fig. 6 is one group of microscope images of the PC-3 cell passage process as it occurs inside the cell culture chamber under 0.4 psi and 0.8 psi peak pressures. In our experiments, pictures were taken every second (here those at 0, 10, 40 and 80 seconds are displayed). As can be seen at 0.4 psi immediately after the diaphragms are activated, shearing forces are applied directly to the cells underneath, detaching them from the surface. The number of cells attached to the surface decreases significantly with time, especially during the initial 10 seconds. As time increases, the rate of cell detachment decreases. At 80 seconds, the majority of cells have been detached, leaving the rest as seeds for the next generation of cells. Afterwards, the number of cells remains constant. Passage at 0.8 psi increases the rate of detachment, leaving fewer cells on the surface. At this point, the diaphragms compress the cancer cells with direct contact, flattening them on the surface, as is clearly visible in the picture at 10 seconds. Reintroducing the detached cells into typical cell culture conditions shows that few of these cells are healthy or viable, due to damage resulting from the hard, shearing forces. The blurs in the picture at 80 seconds are traces of floating cells which move rapidly with diaphragm actuations. A lower gas pressure, such as 0.4 psi, is ideal, not only for keeping cells intact under shearing forces, but also for maintaining an adequate number of cells for repeated culture. After detachment, a higher number of cells stayed in the areas underneath the gaps between two neighboring diaphragms than in those areas underneath the diaphragms (data not shown). For example, at 0.4 psi, 60% of cells might remain attached between the diaphragms, compared to 40% beneath the

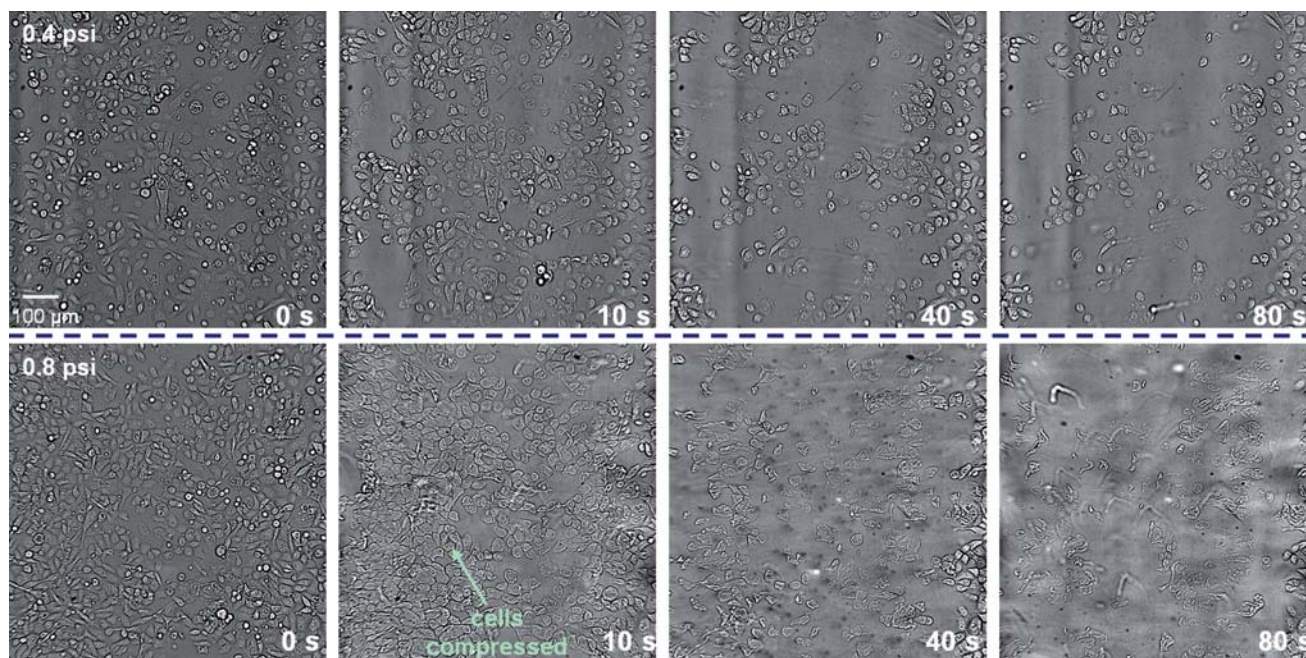


**Fig. 6** PC-3 cell mechanical passage with different gas pressures. The upper panel shows cells passaged using a peak pressure of 0.4 psi; the lower panel shows rapid cell passage at 0.8 psi.

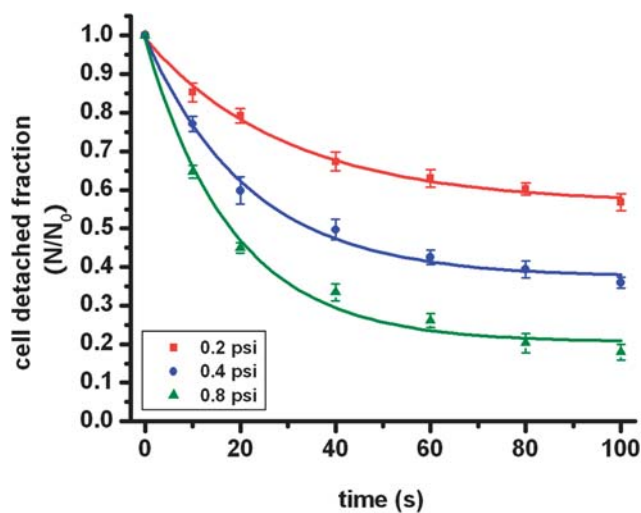


Fig. 7 Fractions of attached cells at various times during passage for gas pressures of 0.2, 0.4 and 0.8. psi.

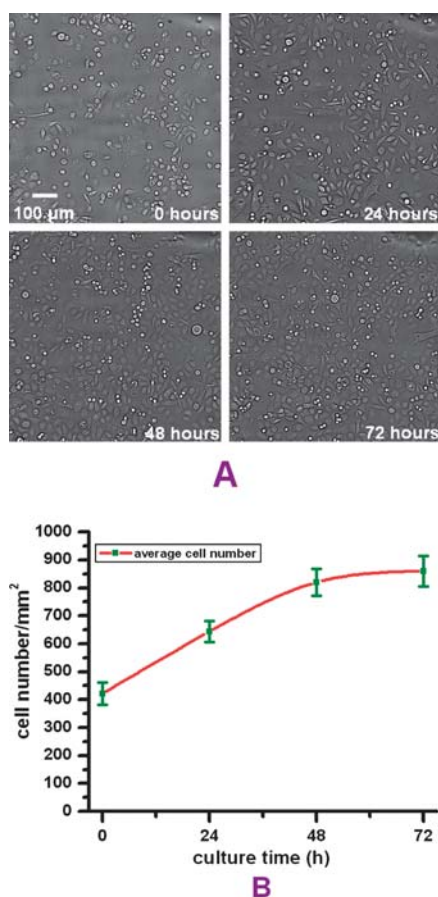


Fig. 8 (A) Microscope images showing PC-3 cells that remained inside the chip continue to grow after mechanical passaging. The culture surface is fully covered with cells within 48 hours. (B) Cell number plotted as a function of time after passage. Green dots are average cell numbers collected from culture chambers in three different chips. Each passage generates more cells than the first culture, and proliferation slows down at 48 hours.

diaphragm. This results from relatively weaker shearing forces between diaphragms, as explained in Fig. 5.

Additional analysis was done to test the chip's capacity for repeated trypsin-free passage. We actuated mechanical passage with gas pressures of 0.2 psi, 0.4 psi and 0.8 psi. We performed three separate passages at each gas pressure using the same cell densities and culture conditions. During the passage process, the number of remaining cells imaged by the microscope was counted and the fraction of attached cells was plotted as a function of elapsed time, as shown in Fig. 7. The data points are average numbers of attached cells at specific times, with error bars representing standard errors of means. The fractions decrease with time, as indicated with colored curves to guide the eye. Thus, according to need, percentages and numbers of "seed" cells can be accurately selected by adjusting the duration of the passage with digital controls.

Viability of cells remaining after passage is a key measure of the chip's ability to be reused for continuous culture. To monitor the ability of the PC-3 cells to regenerate, three chips were passaged under 0.4 psi for 120 seconds and examined afterwards. We counted these cells to derive cell numbers as a function of time. Fig. 8(A) shows a group of cells growing in one location at 0, 24, 48, and 72 hours. In Fig. 8(B), the number of cells averaged across the three chips is plotted as a function of culture time. Error bars show the corresponding standard errors of means. The number of cells remaining after each passage is greater than

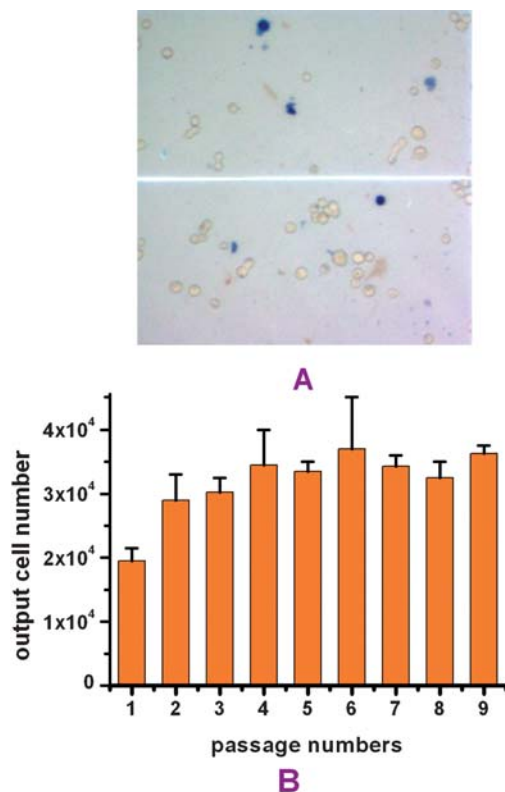


Fig. 9 (A) PC-3 cells passaged for the 9<sup>th</sup> time at 30 days that were collected and tested for viability with trypan blue. The blue cells are dead. The majority of cells are uncolored, indicating they are live. The result shows that the output cells have 97% viability. (B) Output cells counted after each passage.

the number of cells grown from the initial planting, shown in Fig. 3. Cells eventually reached saturation and could be passaged again.

Output cells were also checked for viability. We collected the cells output from the previous passage. We found that these cells were isolated and not clumped. They were mixed with trypan blue (MP biomedical #1691049) at 1 : 1 ratio. After a five minute incubation, the cells were placed in the hemacytometer and observed under a microscope (Fig. 9(A)). The cells in blue color were dead cells, and cells in white were live. We also counted the cells using an automated cell counter (Contess, Invitrogen, Inc). The result shows that, on average, 97% of cells were live.

Long lifetime is another important feature for a culture chip. For this chip, the lifetime is mainly determined by the lifespan of the gelatin coating. To test the longevity of the chips, we used two chips to continuously culture and passage PC-3 cells for 30 days, during which cells were passaged every 3 days (72 hours). The output cells were counted by a hemacytometer (Hausser Scientific, PA). Fig. 9(B) shows that the number of cells output after the first passage was smaller than at the following times (2<sup>nd</sup> through 8<sup>th</sup> passages). This is because cells initially need time to settle down and attach to the surface before they begin to grow. Consequently, cells grow for only part of the first 72 hours. After first passage, cells no longer need time to resettle on the surface. Cells thus have a full 72 hours to grow, leading to greater numbers of output cells than obtained from the first passage. More cells could be easily obtained by adjusting chamber sizes.

## Conclusion

We have introduced a gas controlled microfluidic chip which is able to continuously culture cancer cells *in vitro* and output them externally. Instead of using trypsin as in traditional cell passages, this chip passages cells purely based on shearing forces generated from pneumatic diaphragms. Because the use of trypsin has been avoided, gelatin coatings are no longer depleted during the passage process, so the chip can be reused for subsequent culturing of cells. Requiring fewer reagents during cell culture and passage, the chip has simple operation and robust performance. The electromagnetic valves, together with the digital control box, guarantee not only precise regulation of the number of cells retained for successive cultures, but also the general viability of the output cells. In addition, experiments confirm that the chip can last for at least one month.

Further work is under way including the design and optimization of multiple diaphragms in different sizes with more precise controls. These diaphragms will be employed for studying biophysical behaviors of cells in different passaging stages under adjusted shearing forces. We stress that the functionalities of this

chip are not limited to the cultures and passages of cancer cells, but may also be applicable to other cell types that need to be cultured on similar surfaces. Future directions will focus on integrating multiple cell culture chambers with staggered culture and passage schedules in a single chip. With digital control of syringe pumps, pneumatic valves and mechanical diaphragms, these fully automated cultures and passages will significantly shorten the cell output period from its current 3 days.

## Acknowledgements

We thank Prof. Weijia Wen, Miss Yuling Hua and Prof. Yibin Kang for valuable discussions. The research described was supported by Award Number U54CA143803 from the National Cancer Institute. The content is solely the responsibility of the authors and does not necessarily represent the official views of the National Cancer Institute or the National Institutes of Health.

## References

- 1 A. Jemal, R. Siegel, E. Ward, Y. Hao, J. Xu and M. J. Thun, *Ca-Cancer J. Clin.*, 2009, **59**, 225.
- 2 D. X. Nguyen and J. Massague, *Nat. Rev. Genet.*, 2007, **8**, 341.
- 3 M. E. Kaighn, K. S. Narayan, Y. Ohnuki, J. F. Lechner and L. W. Jones, *Invest. Urol.*, 1979, **17**(1), 16.
- 4 S. Nagrath, L. V. Sequist, S. Maheswaran, D. W. Bell, D. Irimia, L. Ulkus, M. R. Smith, E. L. Kwak, S. Digumarthy, A. Muzikansky, P. Ryan, U. J. Balis, R. G. Tompkins, D. A. Haber and M. Toner, *Nature*, 2007, **450**, 1235.
- 5 K. C. Chaw, M. Manimaran, E. H. Tay and S. Swaminathan, *Lab Chip*, 2007, **7**, 1041.
- 6 C. L. Walsh, B. M. Babin, R. W. Kasinskas, J. A. Foster, M. J. McGarry and N. S. Forbes, *Lab Chip*, 2009, **9**, 545.
- 7 Y. C. Toh, C. Zhang, J. Zhang, Y. M. Khong, S. Chang, V. D. Samper, D. van Noort, D. W. Huttmacher and H. R. Yu, *Lab Chip*, 2007, **7**, 302.
- 8 A. Y. Hsiao, Y. S. Torisawa, Y. C. Tung, S. Sud, R. S. Taichman, K. J. Pienta and S. Takayama, *Biomaterials*, 2009, **30**, 3020.
- 9 P. J. Hung, P. J. Lee, P. Sabounchi, R. Lin and L. P. Lee, *Biotechnol. Bioeng.*, 2005, **89**, 1.
- 10 B. Zhang, M. Kim, T. Thorsen and Z. Wang, *Biomed. Microdevices*, 2009, **11**, 1233.
- 11 L. S. L. Cheung, X. Zheng, A. Stopa, J. C. Baygents, R. Guzman, J. A. Schroeder, R. L. Heimark and Y. Zohar, *Lab Chip*, 2009, **9**, 1721.
- 12 J. V. Green, T. Kniazeva, M. Abedi, D. S. Sokhey, M. E. Taslim and S. K. Murthy, *Lab Chip*, 2009, **9**, 677.
- 13 L. Liu, W. Cao, J. Wu, W. Wen, D. C. Chang and P. Sheng, *Biomicrofluidics*, 2008, **2**, 034103.
- 14 K. J. Regehr, M. Domenech, J. T. Koepsel, K. C. Carver, S. J. Ellison-Zelski, W. L. Murphy, L. A. Schuler, E. T. Alarid and D. J. Beebe, *Lab Chip*, 2009, **9**, 2132.
- 15 L. Liu, X. Niu, W. Wen and P. Sheng, *Appl. Phys. Lett.*, 2006, **88**, 173505.
- 16 A. Mata, A. J. Fleischman and S. Roy, *Biomed. Microdevices*, 2005, **7**, 281.